European Journal of Control (2009)6:649–664

DOI:10.3166/EJC.15.649–664

European Journal of Control

Design of a Fuzzy Multi-objective Power System Stabilizer

M. Soliman[1], A.-L. Elshafei[2,*], F. Bendary[1] and W. Mansour[1]

[1]Electric Power and Machines Department, Faculty of Engineering, Benha University, Cairo 13518, Egypt;
[2]Electric Power and Machines Department, Faculty of Engineering, Cairo University, Giza 12613, Egypt

The design of a model-free fuzzy power system stabilizer (PSS) lacks systematic stability analysis and performance guarantees. This paper provides a step toward the design of a model-based fuzzy PSS that guarantees not only robust stability but also robust performance of power systems. A new practical and simple design based on dynamic output feedback is proposed. The design model is approximated by a set of Takagi-Sugeno (T-S) fuzzy models to account for nonlinearities and uncertainties. The proposed stabilizer is based on parallel distributed compensation (PDC). Sufficient design conditions are presented as linear matrix inequalities (LMIs). The design procedure leads to a tractable convex optimization problem in terms of the stabilizer gain matrices. The design guarantees robust pole clustering, in an acceptable region in the open left half of the complex plane, and robust performance in terms of H_2 and H_∞ measures, over a wide range of operating conditions. Simulations results of both single-machine and multi-machine power systems confirm the effectiveness of the proposed PSS design.

Keywords: Power system dynamic stability, mixed H_2/H_∞ control, linear matrix inequality (LMI), Takagi-Sugeno (T-S) fuzzy models, parallel distributed compensation (PDC)

1. Introduction

Power system stabilizers (PSSs) have been used by utilities to damp out the electromechanical oscillations that follow disturbances [17]. Power systems are often subjected to disturbances due to several reasons, e.g., continuous load variations, set-point changes and faults. In such cases, a fixed-parameter conventional PSS may fail to maintain stability or lead to a degraded performance [5, 18]. Different design techniques such as robust control [16, 25] and adaptive control [11, 23] have been proposed to enhance the performance of PSSs. The implementation of an adaptive controller needs tough precautions to assure persistent excitation conditions and performance merits during the learning phase [23].

Recently, fuzzy logic has emerged as a potential technique for PSS design. Besides its ability to accommodate the heuristic knowledge of a human expert, the advantage of a fuzzy PSS is that it represents a nonlinear mapping that can cope with the nonlinear nature of power systems. Several reported results confirm that a fuzzy PSS outperforms a conventional PSS once the deviation from the nominal design conditions becomes significant [19]. Implementation of a fuzzy PSS for a multi-machine power system is reported in [6]. Tuning the scaling factors of a fuzzy PSS is discussed in [7]. An adaptive PSS using on-line self-learning fuzzy systems is discussed in [1] and on-line tuning of fuzzy PSSs as a direct adaptive one is reported in [8]. Although the performance of a well-designed model-free fuzzy PSS is acceptable, it

*Correspondence to: A.-L. Elshafei, E-mail: elshafei@eng.cu.edu.eg

Received 31 May 2008; Accepted 16 April 2009
Recommended by T. Hikihara, E.F. Camacho

lacks systematic stability analysis and controller synthesis. The reported work attempts to overcome this drawback by a providing a model-based fuzzy PSS that guarantees stability and performance of power systems. In the past ten years, research efforts on fuzzy logic control have been devoted to model-based fuzzy control systems [9]. Stability and performance limits of model-based fuzzy control systems can be achieved via linear matrix inequality (LMI) techniques [28].

LMI techniques are extensively used in the design of a robust PSS, e.g., [2, 21, 22, 30]. In [30], the authors represent the model uncertainty as a linear fractional transformation. An output feedback PSS is designed to guarantee stability for all admissible plants such that a quadratic performance index, based on the nominal plant, is minimized. In [22], pole clustering is used to design a full state feedback for a multi-machine power system. In [21], a combination of LMI and feedback linearization techniques is used to design a centralized PSS for a two-area power system. In [2], a robust decentralized PSS is derived by minimizing a linear objective function under LMI and bilinear matrix inequality (BMI) constraints.

In this paper, an LMI design of a model-based fuzzy dynamic output feedback PSS is proposed. The design guarantees a mix of three relevant objectives for wide range of operating conditions. First, the design guarantees a robust pole clustering in a pre-specified LMI region to maintain adequate damping and better time response. Second, it achieves a good compromise between the control effort and performance by minimizing a certain quadratic performance index (H_2 problem). Third, the design maintains robustness and guarantees disturbance rejection (H_∞ problem). A power system design model is approximated by a poly-topic Takagi-Sugeno (T-S) fuzzy model. Each fuzzy rule (vertex) of the T-S model (poly-tope) represents an extreme operating point corresponding to the selected ranges. According to the universal approximation theorem [28], the resulting fuzzy model can approximate the original nonlinear system to an arbitrary degree of accuracy. A stabilizer design is carried out at each vertex of the poly-tope. The designs are derived under global stability and performance conditions using a common Lyapunov matrix. The design approach leads to a set of LMI conditions. The equivalent control signal is calculated using a parallel distributed compensation (PDC) control law [29].

Up to our knowledge, application of a model-based fuzzy control in PSS design, as proposed here, is a novel approach. Model-based fuzzy control system allows us to use an imprecise design model and consequently, it enables a decentralized design approach that is independent of the power system size as indicated in the following sections. Furthermore, model-based design relies on LMIs rather than BMIs to have a tractable solution.

The rest of the paper is organized as follows. Section 2 describes how to represent an uncertain power system as a poly-topic model that allows for a wide range of operating conditions. In Section 3, a brief review of T-S fuzzy models is depicted followed by the equivalent power system T-S fuzzy model used for PSS synthesis. Section 4 presents the analysis required to describe the conditions for pole clustering, H_2, and H_∞ constraints in an LMI framework. Sufficient LMI conditions required to synthesis the fuzzy dynamic output feedback multi-objective PSS are derived in Section 5. In Section 6, simulation results illustrate the merits of the proposed design. A single-machine infinite-bus system is used first to clarify the design steps. A benchmark model of two-area four-machine test power system is utilized to justify the effectiveness of the decentralized scheme by comparing the proposed PSS to a well-designed conventional PSS and to the standard IEEE PSS4B stabilizer. Section 7 concludes this work.

2. Problem Formulation

In a multi-machine power system, generators are typically equipped with PSSs. To design a local PSS for a generator, we consider an approximate design model that treats the generator as if it was connected to an infinite bus through an equivalent transmission-line reactance. This assumption gets more accurate as the network gets bigger. This can be explained as follows. If a generator is connected to a large network, the transients of the generator do not affect much the rest of the network. So, the network behaves as an infinite bus (i.e., constant voltage and frequency) with respect to that generator. On the other hand, the influence of the network on the generator is reflected on the delivered active and reactive powers. The connection between the generator and the rest of the network is through a Thevenin's equivalent reactance that represents a virtual transmission line. It is apparent that the proposed design model is an approximate representation of the real system. Hence, the proposed control design should rely on robust techniques. First, we will introduce H_∞ and H_2 problems.

Second, we will show how to formulate the PSS design problem in the H_∞ and H_2 framework.

Consider the state space model

$$\begin{aligned} \dot{x} &= Ax + B_1 w + B_2 u \\ y &= C_y x \end{aligned} \tag{1}$$

where x is the state vector, w is the external disturbance, and u is the control signal. The control signal is a supplementary signal added to the excitation system. The system matrices A, B_1, B_2, and C_y have appropriate dimensions. To attenuate the effect of the disturbance w on selected state variables, an auxiliary output z_∞ is introduced as

$$z_\infty = C_1 x \tag{2}$$

where C_1 is a constant matrix of appropriate dimension. The design problem is to select u such that

$$\|z_\infty\|_\infty \leq \gamma \tag{3}$$

where γ is a pre-specified design parameter. It is also frequently required to minimize the total energy of some state variables and the control signal. So, another auxiliary output z_2 is defined as

$$z_2 = C_2 x + D_{22} u \tag{4}$$

where C_2 and D_{22} are constant matrices of appropriate dimensions. This is an H_2 problem that corresponds to the minimization of

$$J = \int_0^\infty \left(x^T R_1 x + u^T R u\right) \mathrm{d}t \tag{5}$$

where R_1 and R are positive definite weighting matrices.

Now, consider the PSS design problem. A typical design model of a single-machine infinite-bus power system is shown in Fig. 1. The state vector is defined as $x = [\Delta\delta \quad \Delta\omega \quad \Delta E_q \quad \Delta E_{fd}]^T$. The state vector is composed of the deviations in power angle $\Delta\delta$, speed $\Delta\omega$, induced voltage ΔE_q, and excitation voltage ΔE_{fd}. The purpose of the PSS is to provide a stabilizing signal u such that the speed deviation $\Delta\omega$ would vanish with an acceptable transient behavior following disturbances. This can be achieved by restricting the closed loop poles within a specified region in the complex plane. Furthermore, if it is required that the maximum $\Delta\omega$ to be less than a certain γ, it is possible to choose

$$z_\infty = \Delta\omega \tag{6}$$

So, any external disturbance that causes $\Delta\omega$ to deviate from zero is regarded as a disturbance. One such example is the change in the excitation reference voltage since it results in some oscillation in $\Delta\omega$. Finally, if it is required to minimize the energy corresponding to $\Delta\omega$ and u, the following H_2 performance index is minimized

$$J = \int_0^\infty \left((\Delta\omega)^2 + r u^2\right) \mathrm{d}t \tag{7}$$

where r is a weighting factor. In such case, the auxiliary output z_2 is

$$z_2 = \left[\Delta\omega \quad \sqrt{r}u\right]^T \tag{8}$$

Combining (1), (2), and (4), the overall design model of a single-machine infinite-bus power system can be cast in the following form

$$\begin{bmatrix} \dot{x} \\ z_\infty \\ z_2 \\ y \end{bmatrix} = \begin{bmatrix} A(k) & B_1 & B_2 \\ C_1 & 0 & 0 \\ C_2 & 0 & D_{22} \\ C_y & 0 & 0 \end{bmatrix} \begin{bmatrix} x \\ w \\ u \end{bmatrix} \tag{9}$$

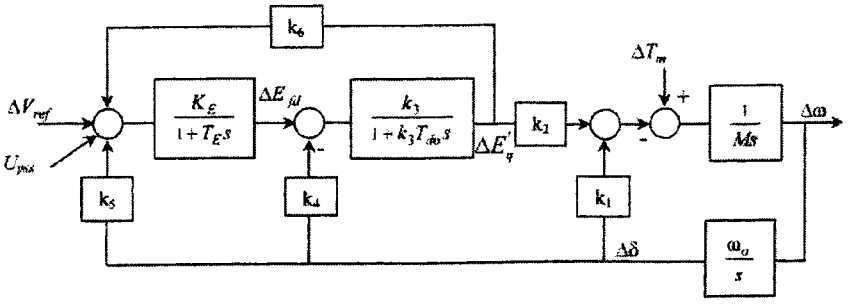

Fig. 1. The linearized model of a single-machine infinite-bus system [5].

where

$$A(k) = \begin{bmatrix} 0 & \omega_o & 0 & 0 \\ -\frac{k_1}{M} & 0 & -\frac{k_2}{M} & 0 \\ -\frac{-k_4}{T_{do}} & 0 & \frac{-1}{T_{do}k_3} & \frac{1}{T_{do}} \\ -\frac{K_E k_5}{T_E} & 0 & -\frac{K_E k_6}{T_E} & -\frac{1}{T_E} \end{bmatrix}$$

$$B_1 = \begin{bmatrix} 0 & 0 & 0 & \frac{K_E}{T_E} \end{bmatrix}^T, B_2 = B_1$$

$$C_1 = \begin{bmatrix} 0 & 1 & 0 & 0 \end{bmatrix}$$

$$C_2 = \begin{bmatrix} 0 & 1 & 0 & 0 \\ 0 & 0 & 0 & 0 \end{bmatrix}$$

$$C_y = \begin{bmatrix} 0 & 1 & 0 & 0 \end{bmatrix}$$

$$D_{22} = \begin{bmatrix} 0 \\ \sqrt{r} \end{bmatrix}$$

The parameters that appear in $A(k)$ and B_1 are defined in the list of symbols; see the Appendix. It is noted that $A(k)$ depends on the so-called k-parameters $(k_1, \cdots, k_6)$ of the model in Fig. 1. These parameters are functions of the delivered active power P and reactive power Q [25]. As P and Q vary, the matrix $A(k)$ varies also. The proposed PSS should stabilize the system over all possible operating points in the ranges $P \in \left[\bar{P}, \overset{+}{P}\right]$ and $Q \in \left[\bar{Q}, \overset{+}{Q}\right]$.

To design a PSS, a T-S fuzzy model is proposed in Section 3. The model consists of IF-THEN rules. The consequents of the rules are the linearized models calculated at $(\bar{P}, \bar{Q})$, $\left(\overset{+}{P}, \bar{Q}\right)$, $\left(\bar{P}, \overset{+}{Q}\right)$, and $\left(\overset{+}{P}, \overset{+}{Q}\right)$. So, the resulting rule base consists of four rules only. The aggregation of the rules form a poly-topic model. The resulting poly-tope has four vertices. Each vertex corresponds to one of the models included in the rule-base. The resulting problem corresponds to stabilizing four plants simultaneously. This can be achieved using the PDC algorithm as explained in Section 3. This is a crucial result as it means that, by stabilizing the fuzzy model, we actually stabilize every model that lies within the poly-tope. So, as long as $P \in \left[\bar{P}, \overset{+}{P}\right]$ and $Q \in \left[\bar{Q}, \overset{+}{Q}\right]$, our design assures stability and performance.

3. T-S Fuzzy Model and PDC

3.1. Review of T-S Fuzzy Systems and PDC

A T-S fuzzy model, also called type-III fuzzy model by Sugeno, is in fact a fuzzy dynamic model [14, 26, 27]. This model is based on using a set of fuzzy rules to describe a global nonlinear system by a set of local linear models which are smoothly connected by fuzzy membership functions. A T-S fuzzy model includes qualitative knowledge, represented by fuzzy IF-THEN rules, and quantitative knowledge, represented by local linear models. The construction of a T-S fuzzy model has been extensively addressed in the literature, e.g., [30] and the references therein. There are two basic approaches to construct T-S fuzzy models. The first approach is to linearize the original nonlinear system at a number of operating points. This approach is adopted in this study since the modeling equations are known. The second approach is based on the data gathered from the nonlinear system when the model is unknown. Based on the first approach, the ith rule of a T-S fuzzy model is written as follows:

Model Rule i:
IF $z_1(t)$ is M_1^i AND ... AND $z_n(t)$ is M_n^i
THEN $\dot{x}(t) = A_i x(t) + B_i u(t)$
$y(t) = C_i x(t)$

$M_j^i, j = 1, 2, \ldots, n$, is the jth fuzzy set of the ith rule and $z_1(t), \ldots, z_n(t)$ are known premise variables that may be functions of state variables, external disturbances, and/or time. Let $\mu_j^i(z_j)$ be the membership function of the fuzzy set M_j^i and let

$$h_i = h_i(t) = \prod_{j=1}^{n} \mu_j^i(z_j) \tag{10}$$

Equation (10) gives ith rule firing strength.

Given a pair $(z(t), u(t))$, the resulting fuzzy system is inferred as the weighted average of the local models and has the following form

$$\begin{aligned} \dot{x} &= \sum_{i=1}^{r} h_i \{A_i x(t) + B_i u(t)\} / \sum_{i=1}^{r} h_i \\ &= \sum_{i=1}^{r} \alpha_i \{A_i x(t) + B_i u(t)\} \\ y &= \sum_{i=1}^{r} \alpha_i \{C_i x(t)\} \end{aligned} \tag{11}$$

where, $\alpha_i = h_i / \sum_{i=1}^{r} h_i$, $0 \le \alpha_i \le 1, \sum_{i=1}^{r} \alpha_i = 1$, for $i = 1, 2, \ldots, r$.

The PDC algorithm offers a procedure to design a fuzzy controller from a given T-S fuzzy model [29]. In the PDC design, each control rule is associated with the corresponding rule of a T-S fuzzy model. The designed fuzzy controller shares the same fuzzy sets with the fuzzy model in the premise parts. For a T-S fuzzy model as described in (11), the following state feedback fuzzy controller is constructed via PDC as follows:

Model Rule # i:

IF $z_1(t)$ is M_1^i AND ... AND $z_n(t)$ is M_n^i

THEN $u(t) = F_i x(t)$, $i = 1, 2, \ldots, r$

The fuzzy control rules have a linear controller in the consequent parts and the overall fuzzy controller is represented by

$$u(t) = \sum_{i=1}^{r} h_i\{F_i x(t)\} / \sum_{i=1}^{r} h_i = \sum_{i=1}^{r} \alpha_i\{F_i x(t)\} \tag{12}$$

Although the fuzzy controller (12) is constructed using local design structures, the feedback gains must be determined using global design conditions to guarantee global stability and performance. Different methods for stability analysis and control design of T-S fuzzy systems are reported in [9]. The analysis adopted in this paper seeks to find a common Lyapunov matrix for all the local subsystems in a T-S fuzzy model.

Substituting (12) into (11), the augmented system is given by

$$\dot{x} = \sum_{i=1}^{r} \sum_{j=1}^{r} \alpha_i \alpha_j \{A_i + B_i F_j\} x(t) \tag{13}$$

Let

$$G_{ij} = A_i + B_i F_j \tag{14}$$

Using (14), it is possible to rewrite (13) as

$$\dot{x} = \sum_{i=1}^{r} \alpha_i^2 G_{ii} x(t) + 2 \sum_{i=1}^{r} \sum_{i<j}^{r} \alpha_i \alpha_j \left(\frac{G_{ij} + G_{ji}}{2}\right) x(t) \tag{15}$$

Theorem 1 [28]: *The T-S fuzzy model (15) is globally asymptotically stable if there exists a common positive definite matrix P such that*

$$G_{ii}^T P + P G_{ii} < 0, \qquad i = 1, 2, \ldots, r \tag{16}$$

$$\left(\frac{G_{ij} + G_{ji}}{2}\right)^T P + P\left(\frac{G_{ij} + G_{ji}}{2}\right) \leq 0, \qquad i < j \tag{17}$$

Corollary 1 [28]: *Assume that $B_i = B, i = 1, 2, \ldots, r$, the equilibrium of the fuzzy control system (17) is globally quadratically stable if a common positive definite matrix P exists and satisfies (16) only. This follows directly because definite negativity of (16) implies semi-definite negativity of (17) in case of common B.*

3.2. A T-S Fuzzy Model for a Single-Machine Infinite-Bus (SMIB) System

It is proposed to represent the SMIB system by the following four-rule T-S fuzzy model.

Model Rule 1:

IF (P is $\bar{P}$) AND (Q is $\bar{Q}$)

$$\text{THEN} \begin{bmatrix} \dot{x} \\ z_\infty \\ z_2 \\ y \end{bmatrix} = \begin{bmatrix} A_1 & B_1 & B_2 \\ C_1 & 0 & 0 \\ C_2 & 0 & D_{22} \\ C_y & 0 & 0 \end{bmatrix} \begin{bmatrix} x \\ w \\ u \end{bmatrix}$$

Model Rule 2:

IF $\left(P \text{ is about } \bar{P}\right)$ AND $\left(Q \text{ is about } \overset{+}{Q}\right)$

$$\text{THEN} \begin{bmatrix} \dot{x} \\ z_\infty \\ z_2 \\ y \end{bmatrix} = \begin{bmatrix} A_2 & B_1 & B_2 \\ C_1 & 0 & 0 \\ C_2 & 0 & D_{22} \\ C_y & 0 & 0 \end{bmatrix} \begin{bmatrix} x \\ w \\ u \end{bmatrix}$$

Model Rule 3:

IF $\left(P \text{ is } \overset{+}{P}\right)$ AND $\left(Q \text{ is } \bar{Q}\right)$

$$\text{THEN} \begin{bmatrix} \dot{x} \\ z_\infty \\ z_2 \\ y \end{bmatrix} = \begin{bmatrix} A_3 & B_1 & B_2 \\ C_1 & 0 & 0 \\ C_2 & 0 & D_{22} \\ C_y & 0 & 0 \end{bmatrix} \begin{bmatrix} x \\ w \\ u \end{bmatrix}$$

Model Rule 4:

IF $\left(P \text{ is } \overset{+}{P}\right)$ AND $\left(Q \text{ is } \overset{+}{Q}\right)$

$$\text{THEN} \begin{bmatrix} \dot{x} \\ z_\infty \\ z_2 \\ y \end{bmatrix} = \begin{bmatrix} A_4 & B_1 & B_2 \\ C_1 & 0 & 0 \\ C_2 & 0 & D_{22} \\ C_y & 0 & 0 \end{bmatrix} \begin{bmatrix} x \\ w \\ u \end{bmatrix}$$

In the above rules, the linguistic variables $\bar{P}$, $\overset{+}{P}$, $\bar{Q}$, and $\overset{+}{Q}$ will be assigned membership functions M_1, M_2, N_1, and N_2, respectively. The construction of the membership functions is given below. The resulting

fuzzy system is inferred as the weighted average of the local models and has the following form:

$$\begin{bmatrix} \dot{x} \\ z_\infty \\ z_2 \\ y \end{bmatrix} = \begin{bmatrix} \sum_{i=1}^{4} \alpha_i A_i & B_1 & B_2 \\ C_1 & 0 & 0 \\ C_2 & 0 & D_{22} \\ C_y & 0 & 0 \end{bmatrix} \begin{bmatrix} x \\ w \\ u \end{bmatrix} \tag{18}$$

Any value $P \in \left[\bar{P}, \overset{+}{P}\right]$ can be expressed as follows:

$$P = M_1(\bar{P}, \overset{+}{P}, P) \times \bar{P} + M_2(\bar{P}, \overset{+}{P}, P) \times \overset{+}{P} \tag{19}$$

where, $M_1(\bar{P}, \overset{+}{P}, P)$ and $M_2(\bar{P}, \overset{+}{P}, P)$ are membership functions of the variable P such that:

$$M_1(\bar{P}, \overset{+}{P}, P) + M_2(\bar{P}, \overset{+}{P}, P) = 1 \tag{20}$$

Consequently, these membership functions can be calculated as:

$$M_1(\bar{P}, \overset{+}{P}, P) = \frac{\overset{+}{P} - P}{\overset{+}{P} - \bar{P}}, \quad M_2(\bar{P}, \overset{+}{P}, P) = \frac{P - \bar{P}}{\overset{+}{P} - \bar{P}} \tag{21}$$

The membership functions for the variable P are shown in Fig. 2. In a similar manner, membership functions for Q are defined and labeled N_1, N_2 respectively. The weights are calculated as follows.

$h_1 = M_2 N_2, h_2 = M_2 N_1, h_3 = M_1 N_2$, and $h_4 = M_1 N_1$. The normalized weights are calculated as $\alpha_i = h_i \Big/ \sum_{i=1}^{4} h_i$, $i = 1, 2, ..., 4$. It is easily proved that $\sum_{i=1}^{4} \alpha_i = 1$.

Remark: *In the proposed modeling approach, each machine is approximated by a separate T-S fuzzy model. As a result of this approach, a multi-machine power system could be decomposed into a set of T-S fuzzy models. This allows for a decentralized design. The interactions between the different T-S fuzzy models are taken into account by a set of scheduling variables (P,Q) that appear in the premise parts of a fuzzy model.*

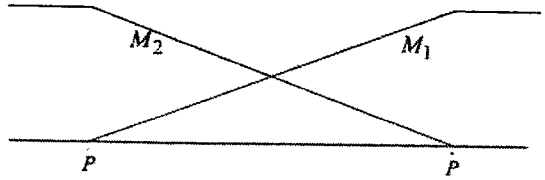

Fig. 2. Membership functions of the scheduling variable P.

4. Performance Requirements of PSS and Their LMI Analysis Conditions

In power systems, a damping ratio of at least 10% and a damping factor greater than 0.5 guarantee that the low frequency oscillations die out in a reasonably short time. These transient response specifications can be satisfied by clustering the closed loop poles in an admissible region as shown in Fig. 3. This ensures a minimum decay rate α_R and a minimum damping $\xi_{\min} = \cos(\theta/2)$. This in turn bounds the maximum overshoot and the settling time of the closed loop system. To avoid very large controller gains, the real part of the poles should be larger than $-\alpha_L$.

The desired multi-objective PSS design must guarantee that all system eigenvalues lie in the pre-described region. This region can be expressed as an LMI region defined by three LMI individual regions as shown in Fig. 3. The intersection of the LMI regions results in another LMI region [3]. An LMI region is any subset D of the complex plane C and it is defined in [3, 4] as follows:

$$D = \{s \in C : \Phi + s\Psi + \bar{s}\Psi^T < 0\} \tag{22}$$

where Φ and Ψ are real matrices, $\Phi = \Phi^T$, and C is the set of complex numbers. In this section, LMI constraints are given to satisfy many design objectives. For the analysis purpose, these inequalities will be written for the closed loop system that has the following state space realization:

$$\begin{aligned} \dot{x} &= A_{cl}x + B_{cl}w \\ z_\infty &= C_{cl\infty}x \\ z_2 &= C_{cl2}x \end{aligned} \tag{23}$$

where A_{cl}, B_{cl}, $C_{cl\infty}$, and C_{cl2} are the closed loop system matrices with appropriate dimension.

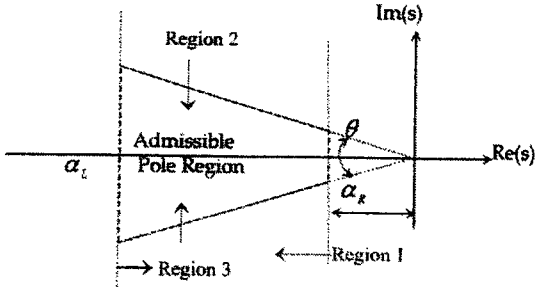

Fig. 3. LMI region: region-1 guarantees an upper bound on the settling time, region-2 guarantees sufficient damping of the system, and region-3 prevents controller gains from being excessively large.

Lemma 1 [3, 4]: *The eigenvalues of system (23) lie inside an LMI region (22), if and only if there is a symmetric positive definite matrix P such that:*

$$\Phi \otimes P + \Psi \otimes (PA_{cl}) + \Psi^T \otimes (A_{cl}^T P) < 0, \tag{24}$$

LMI constraints for the evaluation of the H_2 and H_∞ norm of the closed loop transfer functions from w to z_∞ and z_2 of system (23) defined by $T_{z_\infty w}$ and $T_{z_2 w}$ are provided in [24] and [15]. These LMI conditions are summarized for the sake of completeness in the following lemmas.

Lemma 2 [15, 24]: *The H_∞ norm of the transfer function from w to z_∞ in the system (23) denoted by $\|T_{z_\infty w}\|_\infty$ does not exceed γ_∞ if and only if there exist symmetric positive definite matrix P such that:*

$$\begin{bmatrix} A_{cl}^T P + PA_{cl} & PB_{cl} & C_{cl\infty}^T \\ * & -\gamma_\infty I & 0 \\ * & * & -\gamma_\infty I \end{bmatrix} < 0 \tag{25}$$

Lemma 3 [15, 24]: *The H_2 norm of the transfer function from d to z_2 in system (23) denoted by $\|T_{z_2 w}\|_2$ does not exceed γ_2 if and only if there exist two symmetric matrices P and Q such that:*

$$\begin{bmatrix} A_{cl}^T P + PA_{cl} & PB_{cl} \\ * & -I \end{bmatrix} < 0 \tag{26}$$

$$\begin{bmatrix} Q & C_{cl2} \\ * & P \end{bmatrix} > 0 \tag{27}$$

$$\text{Trace}(Q) < \gamma_2^2 \tag{28}$$

Lemmas 1–3 are used in the following section to design a dynamic output feedback stabilizer satisfying mixed H_2/H_∞ criteria under regional pole constraints.

5. Synthesis of A Fuzzy Multi-Objective Dynamic Output Feedback PSS

In this section, a full order dynamic output feedback fuzzy multi-objective PSS design is proposed. Sufficient LMI conditions for the existence of such PSS are derived. The choice of a particular dynamic PDC parameterization is influenced by the structure of the T-S subsystems [29]. In this paper, linear parameterization is adopted and the proposed model-based fuzzy PSS takes the following form.

$$\begin{aligned} \dot{x}_c &= \sum_{i=1}^{4} \alpha_i \{A_c^i x_c(t) + B_c^i y(t)\} \\ u &= \sum_{i=1}^{4} \alpha_i \{C_c^i x_c(t)\} \end{aligned} \tag{29}$$

where, $x_c \in R^{n\times 1}$ is the controller state vector, $A_c^i \in R^{n\times n}$, $B_c^i \in R^{n\times 1}$, $C_c^i \in R^{1\times n}$ are state space matrices for the ith controller subsystem, and u is the overall control signal. Each rule of the T-S fuzzy model is assigned a local PSS $(A_c^i,\ B_c^i,\ C_c^i)$. The ith control rule is written as

Model Rule i:
IF (P is about $\bar{P}$)AND(Q is about $\bar{Q}$)

$$\text{THEN} \begin{cases} \dot{x}_c = A_c^i x_c + B_c^i y \\ u = C_c^i x_c \end{cases}$$

Define the augmented system matrices for the ith rule as

$$A_{cl}^i = \begin{bmatrix} A_i & B_2 C_c^i \\ B_c^i C_y & A_c^i \end{bmatrix}, B_{cl}^i = \begin{bmatrix} B_1^T & 0 \end{bmatrix}^T,$$

$$C_{cl\infty}^i = \begin{bmatrix} C_1 & 0 \end{bmatrix}, C_{cl2}^i = \begin{bmatrix} C_2 & D_{22} C_c^i \end{bmatrix} \tag{30}$$

The augmented state vector becomes $x_{cl} = \begin{bmatrix} x^T & x_c^T \end{bmatrix}^T$.

A_i is the state matrix of the ith model rule. B_1, B_2, C_1, C_2, C_y, and D_{22} are defined in (9). Substituting (30) in (24)–(26), the resulting synthesis inequalities are not affine in the controller parameters A_c^i, B_c^i, C_c^i and the matrix P. For this reason, the congruence transformation and change of variables presented in [4, 15] are used to have a set of LMIs. The following theorem gives sufficient LMI conditions required to design a model-based fuzzy dynamic output feedback PSS that robustly satisfy the design objectives described in Section 4.

Theorem 2: *The system in (18) is globally quadratically stablizable via the controller (29) and the following objectives:*

- $\sup_{S\in\Omega} \|T_{z_\infty w}\|_\infty < \gamma_\infty$
- $\sup_{S\in\Omega} \|T_{z_2 w}\|_2 < \gamma_2$
- $\mathbf{Eig}(A_{cl}^i) \in D$, where A_{cl}^i is defined in (30) and D is given by (22)

hold if and only if there exist $\mathbf{X} = \mathbf{X}^T, \mathbf{Y} = \mathbf{Y}^T, \mathbf{Q} = \mathbf{Q}^T$ and $\mathbf{A}^i \in R^{nxn}, \mathbf{B}^i \in R^{nx1}$ and $\mathbf{C}^i \in R^{1xn}$ such that for all $i = 1, 2, 3, 4$, the following LMIs hold:

$$\begin{pmatrix} \mathbf{X} & I \\ I & \mathbf{Y} \end{pmatrix} > 0 \tag{31}$$

$$\begin{aligned} \text{P.P}: \Phi \otimes & \begin{pmatrix} \mathbf{X} & I \\ I & \mathbf{Y} \end{pmatrix} \\ + \Psi \otimes & \begin{bmatrix} A_i\mathbf{X} + B_2\mathbf{C}^i & A_i \\ \mathbf{A}^i & \mathbf{Y}A_i + \mathbf{B}^i C_y \end{bmatrix} \\ + \Psi^T \otimes & \begin{bmatrix} A_i\mathbf{X} + B_2\mathbf{C}^i & A_i \\ \mathbf{A}^i & \mathbf{Y}A_i + \mathbf{B}^i C_y \end{bmatrix}^T < 0 \end{aligned} \tag{32}$$

$$\text{H}_\infty: \begin{bmatrix} A_1\mathbf{X} + \mathbf{X}A_i^T + B_2\mathbf{C}^i + \mathbf{C}^{iT}B_2^T & \mathbf{A}^{iT} + A_i & B_1 & \mathbf{X}C_1^T \\ * & \mathbf{Y}A_i + A_i^T\mathbf{Y} + \mathbf{B}^i C_y + C_y^T\mathbf{B}^{iT} & \mathbf{Y}B_1 & C_1^T \\ * & * & -\gamma_\infty I & 0 \\ * & * & * & -\gamma_\infty I \end{bmatrix} < 0 \tag{33}$$

$$H_2: \begin{cases} \begin{bmatrix} A_i\mathbf{X} + \mathbf{X}A_i^T + B_2\mathbf{C}^i + \mathbf{C}^{iT}B_2^T & \mathbf{A}^{iT} + A_i & B_1 \\ * & \mathbf{Y}A_i + A_i^T\mathbf{Y} + \mathbf{B}^i C_y + C_y^T\mathbf{B}^{iT} & \mathbf{Y}B_1 \\ * & * & -I \end{bmatrix} < 0 \\ \begin{bmatrix} \mathbf{Q} & C_2\mathbf{X} + D_{22}\mathbf{C}^i & C_2 \\ * & \mathbf{X} & I \\ * & I & \mathbf{Y} \end{bmatrix} > 0 \\ \text{Trace}(\mathbf{Q}) < \gamma_2^2 \end{cases} \tag{34}$$

Proof: It follows directly from the previous lemmas 1–3 together with the congruence transformation and the change of the variables presented in [4, 15, 24] □.

The decision variables appear in bold letters. The parameters of the ith dynamic controller A_c^i, B_c^i, C_c^i can be recovered again from the new variables $\mathbf{X}, \mathbf{Y}, \mathbf{A}^i, \mathbf{B}^i$, and $\mathbf{C}^i$ as follows:

i. If the set of LMIs given by (31)–(34) is feasible, one can find nonsingular matrices M and N to satisfy that $MN^T = I - \mathbf{XY}$. Schur's complement for LMI (31) infers that $\mathbf{Y} > 0$ and $(\mathbf{X} - \mathbf{Y}^{-1}) > 0$, such that $(I - \mathbf{XY})$ is nonsingular. Hence, two square and nonsingular matrices M and N can be found as a singular value decomposition of the matrix $(I - \mathbf{XY})$.

ii. Using the following correlations between the controller parameters and the new variables for the i^{th} subsystem, one can get the i^{th} controller parameters as

$$C_c^i = \mathbf{C}^i M^{-T} \tag{35}$$

$$B_c^i = N^{-1}\mathbf{B}^i \tag{36}$$

$$A_c^i = N^{-1}\left(\mathbf{A}^i - \mathbf{Y}A_i\mathbf{X} - NB_c^i C_y\mathbf{X} - \mathbf{Y}B_2C_c^i M^T\right)M^{-T} \tag{37}$$

The design steps could be summarized as follows:

i. Determine the ranges $P \in \left[\bar{P} \quad \overset{+}{P}\right]$ and $Q \in \left[\bar{Q} \quad \overset{+}{Q}\right]$ that encompass all practical operating conditions.

ii. Use the ranges in (i) to define the membership functions in (21).

iii. Generate the T-S fuzzy system defined in Subsection 3.2.

iv. Define α_R, α_L, and θ and then find the matrices Φ and Ψ describing the LMI region (24), see [3].

v. Solve the LMI optimization problem in (31)–(34), and use (35)–(37) to get the controller matrices of each rule (vertex).

The above design steps are carried off-line. Using the results of step (v) above, the controller (29) is implemented on-line. Fig. 7 depicts a schematic diagram of the closed loop control system. The controller (29) receives P, Q, and $\Delta\omega$ as inputs and produces the stabilizing signal u as an output.

6. Simulation Results

The proposed PSS design algorithm is validated in this section based on two different models. The first model

is a SMIB model which is used to illustrate the design steps. The second model is a two-area four-machine test power system which is used as a benchmark problem in the literature. In applying the design algorithm to the multi-machine system, each machine is considered as a single machine connected to an infinite bus via a tie line. Consequently, a PSS is designed independently for each machine.

6.1. Design Validation Based on a single-Machine Infinite-Bus Power System

The effectiveness of the proposed stabilizer design method is tested by computer simulation of a nonlinear model given in Appendix A.1. The data are given in Appendix A.2, while generation patterns are assumed to be varying independently over the following intervals:

$$P \in [0.4 \quad 1], \quad Q \in [-0.2 \quad 0.5] \tag{38}$$

These intervals encompass a wide range of operating conditions as it includes different loading conditions such as:

(i) Light loading at leading power factor ($P = 0.4$ pu and $Q = -0.2$ pu)
(ii) Light loading at a poor lagging power factor ($P = 0.4$ pu and $Q = 0.5$ pu)
(iii) Heavy loading at a leading power factor ($P = 1.0$ pu and $Q = -0.2$ pu)
(iv) Heavy loading with lagging power factor ($P = 1.0$ pu and $Q = 0.5$ pu)

Our purpose is to design a fuzzy multi-objective PSS that guarantees a damping ratio of at least 10%, and a damping factor of at least 0.5 for all operating conditions. This objective could be achieved by clustering the closed loop poles inside an LMI region as shown in Fig. 3, where $\alpha_R = -0.5$, $\alpha_L = -15$, and $\theta = 168°$. The LMI region is bounded by α_L to avoid excessive feedback gains and to obtain a better performance formulated in terms of H_∞, H_2, or both. Simulation results are firstly carried out with the open loop system and then the generator is equipped with a fuzzy dynamic output feedback PSS. MATLAB LMI Toolbox [10] is used to solve the Semi-Definite Program (SDP) defined in Theorem 2.

A fine grid is taken for the values of P and Q within the ranges defined in (38) resulting in 1024 plants. The eigenvalues are calculated at each grid point. The dominant poles of these plants are shown in Fig. 4a. Many plants are weakly damped and the others are unstable. This motivates the application of PSS to stabilize all plants and achieve acceptable performance.

Mixed objectives in terms of H_2 and H_∞ under regional pole constraints are considered. Using the ranges of P and Q in (38), a fuzzy model is constructed in the form depicted in Sub-section 3.2. The membership functions are calculated using these bounds as follows:

$$M_1 = \frac{1-P}{0.6}, \quad M_2 = \frac{P-0.4}{0.6},$$
$$N_1 = \frac{0.5-Q}{0.7}, \quad N_2 = \frac{Q+0.2}{0.7}$$

The mixed H_2/H_∞ fuzzy output feedback PSS that guarantees pole clustering is obtained by solving the set of LMIs defined in (31)–(34) such that the objective function $\alpha_1\gamma_\infty + \alpha_2\gamma_2$ is minimized. α_1 and α_2 are two positive scalars used as weights for H_∞ and H_2 costs, respectively. The mixed H_2/H_∞ PSS design guarantees $\gamma_\infty = 0.075$ and $\gamma_2 = 33.3$. The mixed H_2/H_∞ fuzzy output feedback PSS clusters the eigenvalues of all grid points inside the LMI region (27) as shown in Fig. 4b.

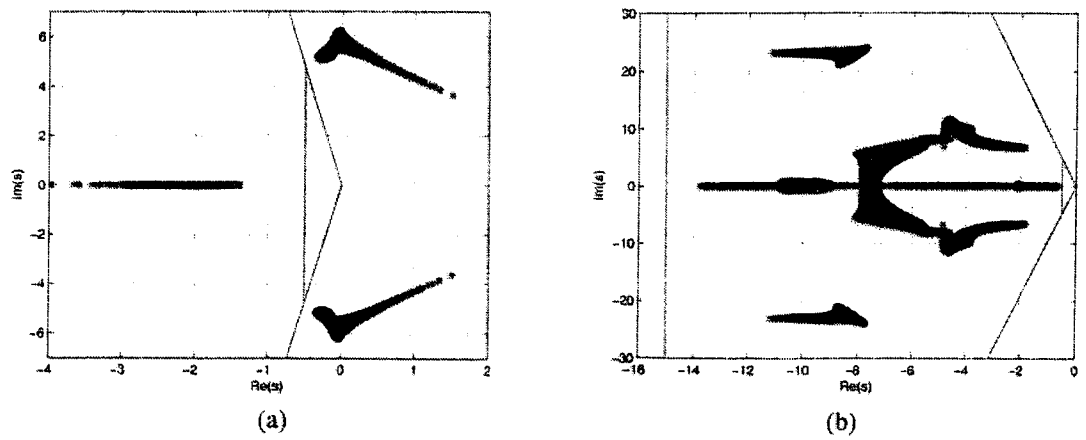

Fig. 4. Pole distribution. (a) Without PSS, (b) with the fuzzy mixed H_2/H_∞ PSS.

The nonlinear model given in Appendix A.1 is used to investigate the performance of the proposed design. The SMIB model is subjected to a small signal disturbance of 3% step change in V_{ref} after 0.5 s, when the generator delivers full load power with unity power factor at generator terminals, i.e., ($P_g = 1.0$ pu, $Q_g = 0.0$ pu). The rotor speed deviation without PSS is depicted in Fig. 5a, while the rotor speed deviation with the proposed fuzzy mixed H_2/H_∞ PSS is depicted in Fig. 5b.

6.2. Design Validation Based on a Multi-Machine Power System

The purpose of this section is to demonstrate the merits of the proposed PSS based on a more realistic model. A benchmark model of a two-area four-machine power system [17] is utilized in this study for the following reasons:

1. It is a multi-machine system that is accepted in the literature as a tool to study the inter-area mode of oscillations.
2. Each generator is represented by a full seventh-order model that considers stator transients and *d-q* damper winding. This makes the results reliable when the system is exposed to large disturbance.
3. This model is available as a Matlab/Simulink demo program [12]. Furthermore, it is equipped with well-tuned PSSs including the standard IEEE PSS4B one [13]. This gives credit to the comparison with the proposed PSS.

The physical system is described in Sub-section 6.2.1. The proposed decentralized algorithm is explained in Sub-section 6.2.2. The design of the proposed PSS is based on a reduced-order model. Another decentralized design is reported in [20]. Finally, in Sub-section 6.2.3, simulation results are depicted. The proposed PSS is compared to the IEEE PSS4B [13] and to Kundur's PSS [17]. Remarkably, the proposed PSS can maintain system stability for extended tie-line power, while IEEE PSS4B and Kundur's PSS could not.

6.2.1. System Description

The two-area four-machine power system, shown in Fig. 6, is adopted for simulation studies. The test system consists of two fully symmetrical areas linked together by two 230 kV lines of 220 km length. It is specifically designed in [17] to study low frequency electro-mechanical oscillations in large interconnected power systems. Each area is equipped with two identical round rotor generators rated 20 kV/900 MVA. The synchronous machines have identical parameters except for the inertias which are H = 6.5 s in area-1 and H = 6.175 s in area-2. Thermal plants having identical speed regulators are further assumed at all locations, in addition to fast static exciter with a gain of 200. The loads are represented as constant impedances and spilt between the areas. The full parameters of a single unit are given in Appendix A.3, while the parameters of the reduced-order model used for design purpose are given in Appendix A.4.

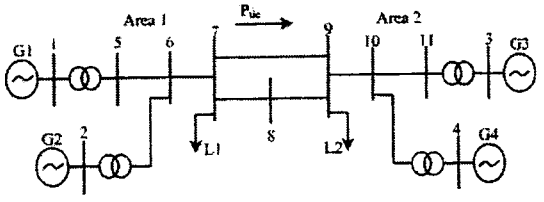

Fig. 6. Two-area four-machine test power system [17].

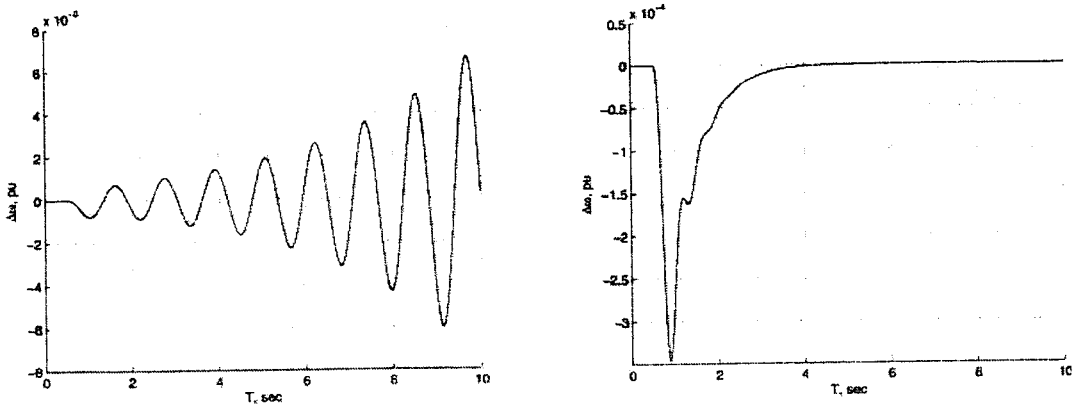

Fig. 5. Rotor speed deviation for 3% step change in V_{ref} at $P_g = 0.9$ pu and $Q_g = 0.0$ pu. (a) Without PSS. (b) With the fuzzy mixed H_2/H_∞ PSS.

6.2.2. PSS Implementation

Fig. 7 shows a schematic diagram of the proposed decentralized PSS design. As explained in Section 2, each generator is approximated by a single-machine infinite-bus model. A local PSS is designed as shown in Sub-section 6.1. The design steps are summarized as follows.

i. Use the load flow studies to determine feasible operating ranges for each generator; i.e., $P_i \in \left[\bar{P}_i \quad \overset{+}{P}_i\right]$ and $Q_i \in \left[\bar{Q}_i \quad \overset{+}{Q}_i\right]$ for $i=1, 2,..., 4$ where i is the generator index.
ii. Calculate the bus impedance matrix to determine approximate values of the reactance that connect each generator to the infinite bus.
iii. Construct a fuzzy model (as shown in Sub-section 3.2) for each generator.
iv. Define an LMI region similar to that in Fig. 3 to encompass the closed loop poles and guarantee acceptable transient response.
v. Solve the LMIs (31)–(34) for each generator and use (35)–(37) to construct the controller as depicted in Section 5.
vi. Implement the control law (29).

6.2.3. Simulation Results

The tie-line power of the test system is assumed to vary between 200 and 800 MW. A fine grid of tie-line power is assumed and 25 grid points are considered. Each grid point should have a steady-state load flow solution. The roots of the linearized system at different grid points are calculated and the dominant modes are shown in Fig. 8a. The dominant roots include two sets of oscillation modes namely, local and inter-area modes. Many grid points are unstable due to inter-area oscillations. A mixed H_2/H_∞ fuzzy PSS is designed for each machine separately and the roots of the closed loop system are calculated at each grid point and plotted as shown in Fig. 8b. The proposed PSS gives sufficient damping over both local and inter-area modes of oscillations.

A comparison between the conventional PSS [17], the standard IEEE PSS4B [13] and the proposed design is carried out. To check the effectiveness of the proposed PSS to improve transient stability and extend the stability margin of power systems, two levels of tie-line powers are tested and different fault conditions are considered. The following points consider system response due to a three-phase short circuit at different locations under different values of tie-line power.

i. When area-1 delivers 413 MW to area-2, the system undergoes a large disturbance of a three phase to ground fault at bus-8 and cleared by tripping the breaker at the ends of the lines connected to bus-8 after 133 ms. Relative speed and relative angle between machine -1 and machine -4 are shown in Fig. 9a,b, while the tie-line power is depicted in Fig. 9c. It is obvious that the proposed design outperforms both CPSS and IEEE PSS4B at this point

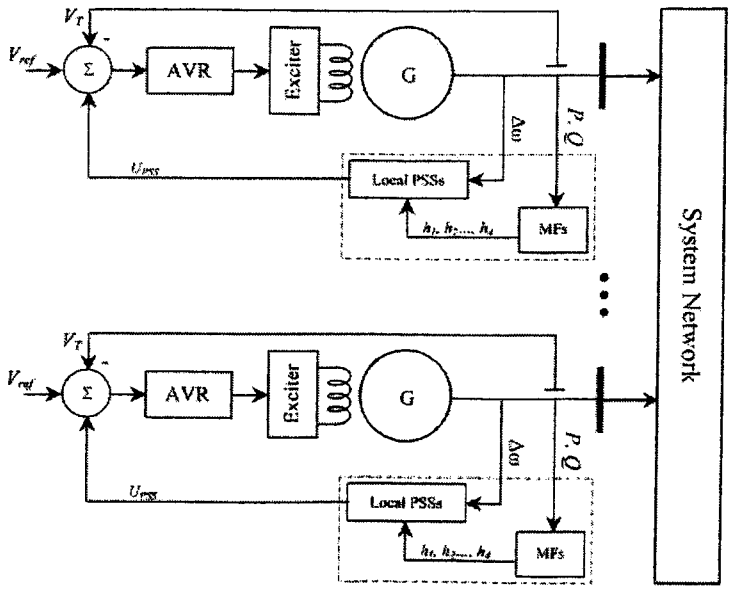

Fig. 7. Fuzzy synthesis framework for decentralized PSS design.

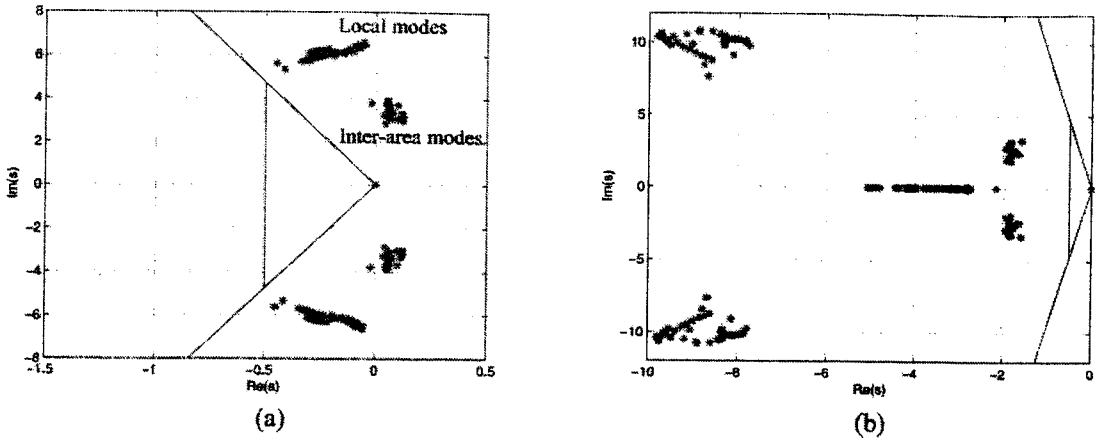

Fig. 8. Dominant poles. (a) Without PSS. (b) With fuzzy mixed H_2/H_∞ PSS.

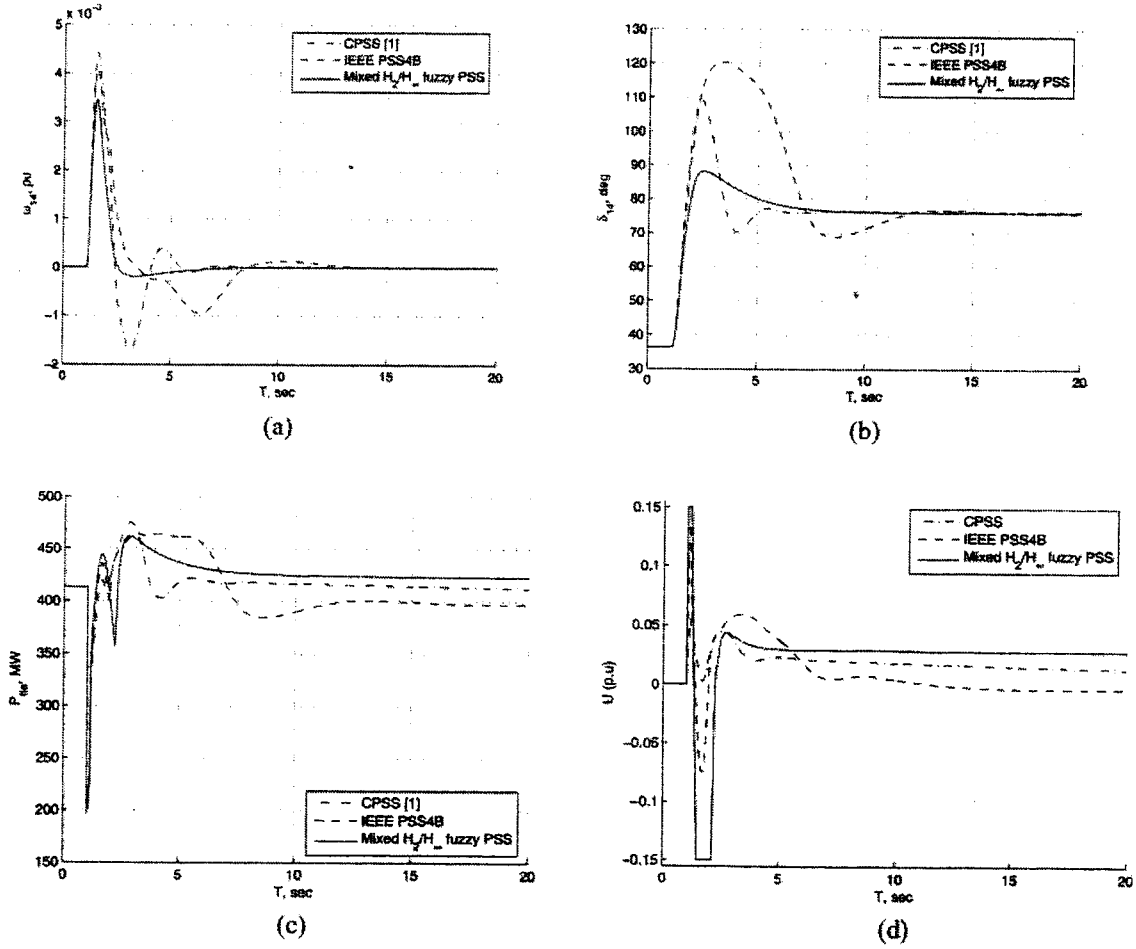

Fig. 9. System response due to a 3-phase short circuit at bus-8 cleared after 133 m ($P_{tie} \approx 410$ MW).

which is considered as the nominal design point for the CPSS.

ii. When area-1 delivers about 450 MW to area-2, the system undergoes a three-phase short circuit at bus-8 and cleared by tripping the breakers at ends of the lines connected to bus-8 after 133 ms. The conventional PSS and the IEEE PSS4B fail to maintain system stability at this increased tie-line power. The proposed PSS succeeds to do that. The system response at this operating point is depicted in Fig. 10. The control signal is as shown in Fig. 10d.

Assume a three-phase short circuit occurs at 90 km far from area-2, under the same tie-line power ($P_{tie} \approx 450$). Both CPSS and IEEE PSS4B fail to maintain stability, while the proposed fuzzy PSS succeeds as depicted in Fig. 11.

Remarks:

The above design assumes that the LMI conditions (31)–(34) are feasible. For some ranges of P and Q or even for some values of the machine parameters, the LMI solver may fail to find a feasible solution. In such

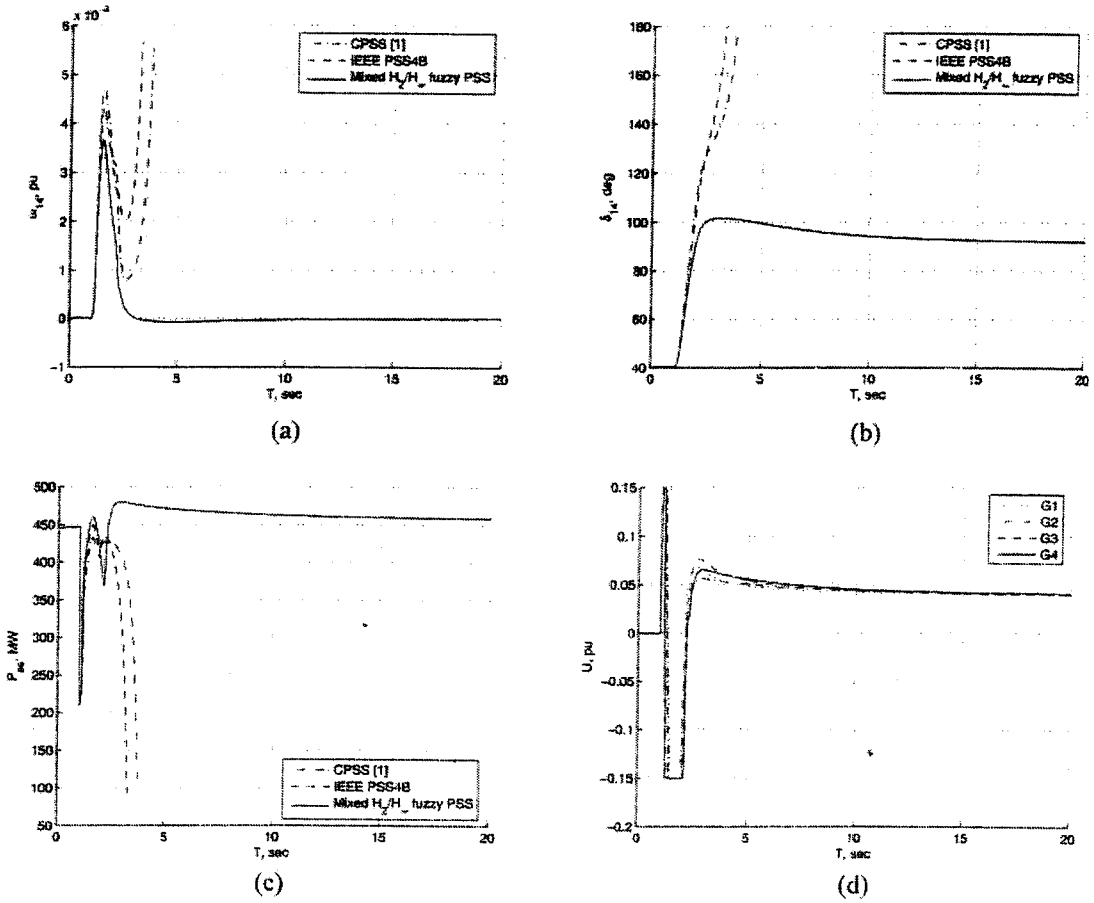

Fig. 10. System response due to a 3-phase short circuit at bus-8 cleared after 133 m. ($P_{tie} \approx 450$ MW). (a) Relative speed between machine-1 and machine-4. (b) Relative angle between machine-1 and machine-4. (c) Tie line power. (d) Control signals provided by the proposed design.

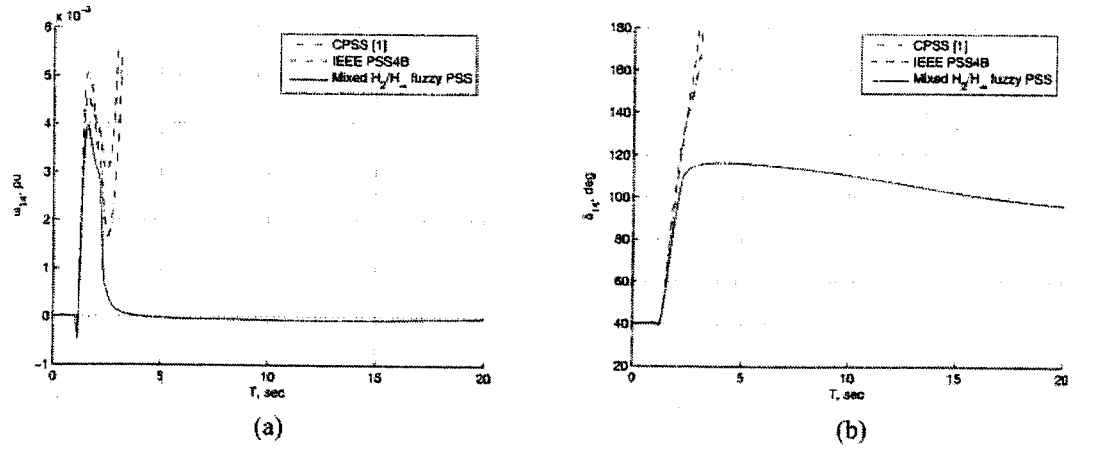

Fig. 11. System response due to a 3-phase short circuit at 90 km far from area-2, cleared after 133 m. ($P_{tie} \approx 450$). (a) Relative speed between machine-1 and machine-4. (b) Relative angle between machine-1 and machine-4.

cases, the design ranges of P and Q could be made narrower or the design could be based on relaxed stability conditions [9]. Lastly, if the LMI conditions remain infeasible, another design algorithm is adopted. The superiority of the proposed controller can be explained as follows:

a. *It imitates a smooth gain scheduling design algorithm where a different controller is actually applied according to the need of the plant. The transition from one controller to another is smooth since it is carried out via a fuzzy system.*
b. *Fuzzy controllers are nonlinear mappings while the CPSS and IEEE PSS4B are linear ones. This nonlinearity gives more flexibility in shaping the control surface and producing better performance.*

7. Conclusions

A design of a PSS that can cope with a wide range of loading conditions and external disturbances has been the objective of the power industry. This paper has provided a step toward this goal. It has been shown that the nonlinear model of a power system can be systematically represented by a poly-topic model in the form of a T-S fuzzy system. A multi-objective criterion including robust pole clustering, limited control energy, and pre-specified attenuation of the disturbance effect has been introduced for dynamic output feedback case. Sufficient LMI conditions have been derived for control synthesis. These LMI conditions have been efficiently solved using the interior point algorithm. The resulting controller has been implemented based on the PDC approach. Simulation results of a two-area four-machine power system have confirmed the superiority of the proposed algorithm in damping the post-fault inter-area oscillations. Compared to a well-tuned conventional PSS and to the IEEE PSS4B, it has been shown that the proposed PSS has a superior capability to cope with larger tie-line power.

References

1. Abdelazim T, Malik OP. An adaptive power system stabilizer using on-line self-learning fuzzy systems. In Proceedings of the IEEE Power Engineering Society General Meeting, Toronto, ON, Canada, 2003, pp. 1715–1720
2. Befekadu GK, Erlich I. Robust decentralized controller design for power systems using matrix inequalities approaches. In IEEE/PES General Meeting, 2006, pp. 18–22
3. Chilali M, Gahinet P, Apkarian P. Robust pole placement in LMI regions. *IEEE Trans Autom Control* 1999; 44: 2257–2270
4. Chilali M, Gahinet P. H_∞ design with pole placement constraints: an LMI approach. *IEEE Trans Autom Control* 1996; 41: 358–367
5. DeMello FP, Concordia C. Concepts of synchronous machine stability as affected by excitation control. *IEEE Trans Power Appar Syst* 1969; PAS-88: 316–329
6. El-Metwally K, Malik OP. Application of fuzzy-logic stabilizers in a multi-machine environment. *IEE Proc Gener Transm Distrib* 1969; 143: 263–268
7. El-Metwally K, Malik OP. Parameter tuning for fuzzy logic control. In Proceedings of the IFAC World Congress on Automation and Control, Sydney, 1993, pp. 581–584
8. Elshafei AL, El-Metwally K, Shaltout A. A variable-structure adaptive fuzzy-logic stabilizer for single and multi-machine power systems. *Control Eng Pract* 2005; 13: 414–423
9. Feng G. A survey on analysis and design of model-based fuzzy control systems. *IEEE Trans Fuzzy Syst* 2006;14: 676–697
10. Gahinet P, Nemirovski A, Laub A, Chilali M. *LMI Control Toolbox*, The Math Works, Natick, MA, 1995
11. Ghosh A, Ledwich A, Malik O, Hope G. Power system stabilizers based on adaptive control techniques. *IEEE Trans Power Appar Syst* 1984; 103:1983–1989
12. Hydro-Quebec, TEQSIM International, Power System Blockset, Math Works Inc., 1998
13. IEEE Power Engineering Society, IEEE Recommended Practice for Excitation System Models for Power System Stability Studies, IEEE Std 421.5®-2005–2006
14. Johansen T, Shorten R, Murray-Smith R. On the interpretation and identification of dynamic Takagi–Sugeno models. *IEEE Trans Fuzzy Syst* 2000; 8: 297–313
15. Kanev S, Scherer C, Verhaegen M, De Schutter B. Robust output feedback controller desgin via local BMI optimazition. *Automatica* 2004; 40: 1115–1127
16. Klein M, Le L, Rogers G, Farrokhpay S, Balu NJ. H_∞ damping controller design in large power systems. *IEEE Trans Power Appar Syst* 1995; 10: 158–165
17. Kunder P. *Power System Stability and Control*, McGraw Hill, New York, 1994
18. Larsen EV, Swann DA. Applying power system stabilizers, Parts I, II, III. *IEEE Trans Power Appar Syst* 1981; PAS-100: 33017–3046
19. Malik OP, El-Metwally K. Fuzzy logic controllers as power system stabilizers. In: El-Hawary M (ed), *Electric Power Applications of Fuzzy Logic*, IEEE Press, New York, 1998, pp. 112–148
20. Qiu W, Vittal V, Khammash M. Decentralized power system stabilizer design using linear parameter varying approach. *IEEE Trans Power Syst* 2004; 19: 1951–1960
21. Ramos RA, Alberto LF, Bretas NG. Linear matrix inequality based controller design with feedback linearization: application to power systems. *IEE Proc Control Theory Appl* 2003; 150: 551–556
22. Rao PS, Sen I. Robust pole placement stabilizer design using linear matrix inequalities. *IEEE Trans Power Appar Syst* 2000; 15: 313–319

23. Sastry S, Bodson M. *Adaptive Control: Stability, Convergence, and Robustness*, Prentice Hall, Englewood Cliffs, NJ, 1989
24. Scherer C, Gahinet P, Chilali M. Multi-objective output-feedback control via LMI optimization. *IEEE Trans Autom Control* 1997; 42: 896–911
25. Soliman H, Elshafei AL, Shaltout A, Morsi M. Robust power system stabilizer. *IEE Proc Electr Power Appl* 2000; 147: 285–291
26. Sugeno M, Kang GT. Structure identification of fuzzy model. *Fuzzy Sets Syst* 1986; 28: 329–346
27. Takagi T, Sugeno M. Fuzzy identification of systems and its applications to modeling and control. *IEEE Trans Syst Man Cybern* 1985; 15: 116–132
28. Tanaka K, Wang HO. *Fuzzy Control Systems Design and Analysis: A Linear Matrix Inequality Approach*, John Wily & Sons, New York, 2001
29. Wang HO, Tanaka K, Griffin MF. Parallel Distributed Compensation of Nonlinear Systems by Takagi-Sugeno Fuzzy Model. In Proceedings of FUZZ-IEEE/IFES'95, 1995, pp. 531–538
30. Werner H, Korba P, Chen Yang T. Robust Tuning of Power System Stabilizers Using LMI Techniques. *IEEE Trans Control Syst Technol* 2003; 11: 147–2003

Appendix 1

A.1 Nonlinear 4th order SMIB model (design model)

$$\dot{\delta} = \omega_o \omega$$

$$\dot{\omega} = \frac{1}{M}\left[T_m - \left(\frac{V_\infty}{(x_e + x'_d)}\right) E'_q \sin\delta + \left(\frac{(x_q - x'_d)V_\infty^2}{2(x_e + x'_d)(x_e + x_q)}\right)\sin 2\delta\right]$$

$$\dot{E}'_q = \frac{1}{T'_{do}}\left[-\left(\frac{x_e + x_d}{x_e + x'_d}\right)E'_q + \left(\frac{x_d - x'_d}{x_e + x'_d}V_\infty\right)\cos\delta + E_{fd}\right]$$

$$\dot{E}_{fd} = \frac{K_E}{T_E}\left(V_{REF} + u - \sqrt{c_0 + c_1\cos^2\delta + c_2 E'_q \cos\delta + c_3 E'^2_q}\right) - \frac{1}{T_E}E_{fd}$$

$$c_0 = \left(\frac{x_q V_\infty}{x_e + x_q}\right)^2,\quad c_1 = \left[\left(\frac{x'_d V_\infty}{x_e + x'_d}\right)^2 - \left(\frac{x_q V_\infty}{x_e + x_q}\right)^2\right],$$

$$c_2 = \left[\frac{2x_e x'_d V_\infty}{(x_e + x'_d)^2}\right],\quad c_3 = \left(\frac{x_e}{x_e + x'_d}\right)^2$$

A.2 Data of the SMIB model used in simulation in Sub-section 6.1.

$$x_d = 1.6, x_q = 1.55, x'_d = 0.32, T'_{do} = 6,$$
$$M = 10, K_E = 25, T_E = 0.05, E_{fd\,min} = -5,$$
$$E_{fd\,max} = 5, U_{min} = -0.1\,\text{pu}, U_{max} = 0.1\,\text{pu},$$
$$V^\infty = 1, \omega_o = 314, \text{ Rating} = 100\,\text{MVA}$$

The vertices of the SMIB poly-tope

$$A_1 = \begin{bmatrix} 0 & 314.16 & 0 & 0 \\ -0.0896 & 0 & -0.1226 & 0 \\ -0.2616 & 0 & -0.4629 & 0.1667 \\ -24.816 & 0 & -172.24 & -20 \end{bmatrix}$$

$$A_2 = \begin{bmatrix} 0 & 314.16 & 0 & 0 \\ -0.1038 & 0 & -0.0569 & 0 \\ -0.1213 & 0 & -0.4629 & 0.1667 \\ -14.161 & 0 & -266.67 & -20 \end{bmatrix}$$

$$A_3 = \begin{bmatrix} 0 & 314.16 & 0 & 0 \\ -0.0221 & 0 & -0.1249 & 0 \\ -0.2664 & 0 & -0.4629 & 0.1667 \\ 199.31 & 0 & -37.294 & -20 \end{bmatrix}$$

$$A_4 = \begin{bmatrix} 0 & 314.16 & 0 & 0 \\ -0.1248 & 0 & -0.1186 & 0 \\ -0.2531 & 0 & -0.4629 & 0.1667 \\ 24.273 & 0 & -220.11 & -20 \end{bmatrix}$$

$$B_i = B = \begin{bmatrix} 0 \\ 0 \\ 0 \\ 500 \end{bmatrix}, i = 1, \ldots, 4,$$

$$C_i = C = [0 \quad 1 \quad 0 \quad 0], i = 1, \ldots, 4$$

Table 1. Initial states of the nonlinear model calculated at the test point $P = 0.9$, pu, $Q = 0$pu

	P	Q	Terminal voltage (V_T)	Initial states
Test point	0.9	0.0	$0.9203\angle 23.03°$	$\Delta\omega = 0, \delta_0 = 81.761,\ E'_{q0} = 0.79451$ pu, $E_{fd0} = 1.8151$ pu

A.3 The full parameters of one unit of the test system given in [17].

$$R_a = 0.0025,\ x_d = 1.8,\ x_q = 1.7,\ x_\ell = 0.2,$$
$$x'_d = 0.3,\ x'_q = 0.55,\ x'_d = x'_q = 0.25$$
$$T'_{do} = 8.0,\ T'_{qo} = 0.4,\ T''_{do} = 0.03,\ T''_{qo} = 0.05,$$
$$H = 6.5,\ \omega_o = 376.99\,\text{rad/s},$$
$$\text{RATING} = 900\,\text{MVA},\ K_E = 200,\ T_E = 0.001,$$
$$E_{fd\,min} = 0,\ E_{fd\,max} = 12.3\,\text{pu},$$
$$U_{min} = -0.15\ \text{pu},\ U_{max} = 0.15\,\text{pu}.$$

A.4 The parameters of the approximate 4th order model used for design purpose only in Sub-section 6.2.

$$x_d = 1.8, x_q = 1.7, x'_d = 0.3, T'_{do} = 8.0, M = 13,$$
$$K_E = 200,\ T_E = 0.001$$
$$\omega_o = 376.99\,\text{rad/sec}, \text{RATING} = 900\,\text{MVA}$$

A.5 Load flow data for the test points in Sub-section 6.2.3 (Tables 2–3).

A.6 List of symbols:

All quantities are in pu except M is in seconds, time constants are in seconds and δ is in radians:

V_t = terminal voltage
E_q = induced EMF proportional to field current
E_{fd} = generator field voltage
V_{ref} = reference voltage
x_e = tie line reactance
x'_d, x_d, x_q = generator d-axis transient reactance, d and q-axes synchronous reactance, respectively
δ = angle between q-axis and infinite-bus bar
I_d, I_q = d-axis and q-axis stator currents
$\Delta\omega$ = speed deviation
ω_o = synchronous speed (rad/s)
T_e = electrical torque
T_m = mechanical torque
T'_{d0} = open-circuit d-axis transient time constant
M = inertia coefficient in seconds
K_E, T_E = exciter gain and time constant
V^∞ = infinite-bus voltage
P, Q = active and reactive power loading, respectively
s, C = complex operator and complex plane, respectively
$\otimes$ = Kronecker product
Trace = trace of a matrix
* = ellipses for symmetry in off-diagonal entries of a matrix

Table 2. Test point 1 for the system in Fig. 6 (all value are given in per unit)

Bus index	Generation (P + jQ)	Loads (P + jQ)	Bus voltages
1	0.7778 + j0.1725	–	1∠28.18°
2	0.7778 + j0.3051	–	1∠17.73°
3	0.8030 + j0.1636	–	1∠0°
4	0.7778 + j0.2678	–	1∠ − 10.98°
5	–	–	0.9811∠21.35°
6	–	–	0.9613∠10.76°
7	–	1.0744 − j 0.1111	0.945∠2.05°
8	–	–	0.9555∠ − 26.64°
9	–	1.9633 − j 0.2778	0.9667∠ − 17.91°
10	–	–	0.983∠ − 7.0396°

Table 3. Test point 2 for the system in Fig. 6 (all value are given in per unit)

Bus index	Generation (P + jQ)	Loads (P + jQ)	Bus voltages
1	0.7889 + j0.1864	–	1∠27.51°
2	0.7889 + j0.3337	–	1∠16.88°
3	0.90414 + j0.2205	–	1∠0°
4	0.7778 + j0.3367	–	1∠ − 13.43°
5	–	–	0.9792∠20.57°
6	–	–	0.9573∠9.78°
7	–	1.0744 − j 0.1111	0.938∠0.87°
8	–	–	0.942∠ − −29.92°
9	–	2.0744 − j 0.2778	0.9566∠ − −20.43°
10	–	–	0.976∠ - - 7.98°